nature chemistry

ARTICLES

PUBLISHED ONLINE: 2 FEBRUARY 2015 | DOI: 10.1038/NCHEM.2173

Atropselective syntheses of (−) and (+) rugulotrosin A utilizing point-to-axial chirality transfer

Tian Qin[1], Sarah L. Skraba-Joiner[2], Zeinab G. Khalil[3], Richard P. Johnson[2], Robert J. Capon[3] and John A. Porco Jr[1]*

Chiral, dimeric natural products containing complex structures and interesting biological properties have inspired chemists and biologists for decades. A seven-step total synthesis of the axially chiral, dimeric tetrahydroxanthone natural product rugulotrosin A is described. The synthesis employs a one-pot Suzuki coupling/dimerization to generate the requisite 2,2′-biaryl linkage. Highly selective point-to-axial chirality transfer was achieved using palladium catalysis with achiral phosphine ligands. Single X-ray crystal diffraction data were obtained to confirm both the atropisomeric configuration and absolute stereochemistry of rugulotrosin A. Computational studies are described to rationalize the atropselectivity observed in the key dimerization step. Comparison of the crude fungal extract with synthetic rugulotrosin A and its atropisomer verified that nature generates a single atropisomer of the natural product.

As a consequence of the hindered rotational barriers of highly substituted biaryls and related compounds, a type of stereochemistry in the form of axial chirality is generated, often termed atropisomerism[1]. Atropisomerism exists widely in nature and can lead to biological stereoselectivity for molecular targets[2–4]. Moreover, in contrast to traditional sp^3 carbon-centred chirality, control of axial chirality and atropisomer selectivity remains highly challenging, especially in the context of complex natural product synthesis[5–8].

Tetrahydroxanthones[9]—secondary fungal metabolites—are an emerging family of natural products. Dimeric tetrahydroxanthones[10] including the secalonic acids[11,12] (Fig. 1a) display intriguing anticancer and antibacterial properties. During the last decade, tetrahydroxanthones containing biaryl axial chirality including the 2,2′-linked natural product[13] rugulotrosin A (**1**) and the 2,4′-linked congener rugulotrosin B (**2**) (Fig. 1b) have been isolated and characterized. Related hybrid chromone lactone/tetrahydroxanthones including the 2,4′-linked heterodimer gonytolide E (**3**)[14] and the 4,4′-linked chromone lactone homodimer gonytolide A (**4**)[15] have also been reported. Recently, these interesting molecules have attracted significant interest in the synthetic community, as evidenced by reports of syntheses of both monomeric[16–22] and dimeric natural products[23]. However, syntheses of tetrahydroxanthones bearing axial chirality, such as rugulotrosin A (**1**) and related compounds, have not been reported.

To establish axial chirality for rugulotrosin A, we envisioned that a point-to-axial chirality transfer strategy could be implemented. In the last few decades, point-to-axial chirality transfer has been widely used in atropselective synthesis. There are several different approaches to point-to-axial chirality transfer: (1) the use of an *ortho*-auxilary[5,6] or chiral leaving group[24] for intermolecular, atropselective coupling; (2) utilization of low-energy conformers derived from existing chirality centres[25,26] or chiral auxiliaries[5,6] to execute intramolecular couplings; (3) transfer of chiral sp^3 carbon to axial chirality[27,28]; and (4) the use of remote and existing chirality centres to influence atropselectiviy using intermolecular oxidative/metal-mediated couplings[29–33]. Shaw and colleagues, for example, have reported that the chiral monomer **5** underwent oxidative coupling to generate atropisomer **6** in 76:24 diastereomeric ratio (d.r.), which could be improved to higher selectivity using a chiral catalyst system[29] (Fig. 1c). Similarly, Lipshutz and co-workers performed an atropselective cross-coupling to access the korupensamine B precursor **9** using boronic acid **7** and iodotetrahydroisoquinoline partner **8**[31] (Fig. 1c). In the present studies we considered a remote asymmetric induction strategy for point-to-axial chirality transfer for rugulotrosin synthesis in the absence of chiral auxiliaries. In the case of dimerization of tetrahydroxanthone substrate **10**, it was of interest to determine whether the chirality of the remote stereocentres could be transferred to the axial chirality of *ortho*, *ortho* dimer **11** (Fig. 1d), a product bearing a coupling pattern different from those of previous examples. In this case we planned to make use of transition-metal catalysis to bring the two monomers in close proximity to enhance the potential for chirality transfer.

Results and discussion

Our synthesis was initiated with chromone **12**, which was prepared in greater than 50 g batches and purified by recrystallization (Fig. 2). Utilizing diisopropylsilyl ditriflate to activate chromone **12** to a siloxybenzopyrylium species[22], vinylogous addition of 2-trimethylsiloxyfuran was achieved, which was followed by hydrogenation to afford chromone lactone **13** on a decagram scale (89% yield, d.r. > 10:1) after purification by trituration (Supplementary pages 4–19). Further treatment of **13** with NaH in THF led to the production of *epi*-blennolide C **14** through Dieckmann cyclization. Due to the propensity of the vinylogous acid moiety of tetrahydroxanthone **14** to both epimerization and tetrahydroxanthone-to-chromone lactone rearrangement, we utilized the neutral methylating

[1]Department of Chemistry and Center for Molecular Discovery (BU-CMD), Boston University, Boston, Massachusetts 02215, USA. [2]Department of Chemistry, University of New Hampshire, Durham, New Hampshire 03824, USA. [3]The University of Queensland, Institute of Molecular Bioscience, 306 Carmody Road, St Lucia, Queensland 4072, Australia. *e-mail: porco@bu.edu

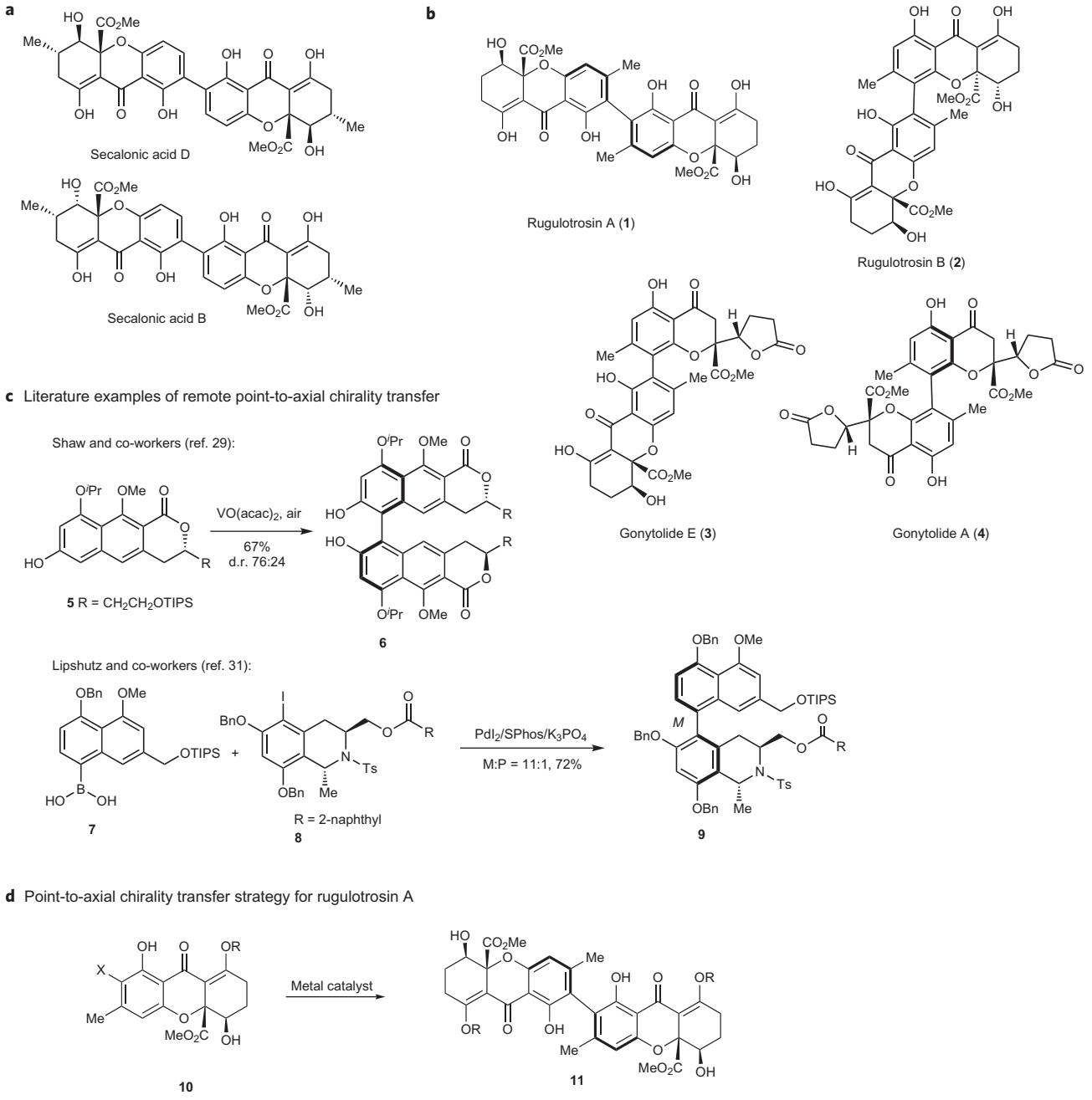

Figure 1 | Axially chiral, dimeric tetrahydroxanthone natural products and point-to-axial chirality transfer strategy. a, Structures of the dimeric tetrahydroxanthone natural products secalonic acids B and D. **b**, Structures of representative axially chiral tetrahydroxanthone natural products. **c**, Select literature examples of remote point-to-axial chirality transfer. **d**, Strategy for the synthesis of rugulotrosin A.

reagent trimethylsilyldiazomethane to obtain the desired *O*-methylated product **16** in 61% yield as well as the separable isomer **15** (20% yield). After phenol-directed *ortho*-iodination of **16**, the derived aryl iodide **17** was subjected to kinetic acylative resolution using Birman's catalyst[34] on a gram scale (selectivity (s) factor >200)[35]. Chiral monomer (−)-**17** was isolated in 46% yield (99% enantiomeric excess (e.e.)) and the *O*-acylated product (+)-**18** was obtained in 46% yield (99% e.e.) after recrystallization.

After obtaining the two enantiopure tetrahydroxanthone monomers, our initial plan was to make use of our stannane dimerization strategy, which successfully led to syntheses of secalonic acids A and D[23]. However, after evaluation of various conditions, we observed only trace stannylation of iodides **17** or **18** (Table 1), which may be due to steric hindrance of the aryl iodide substrate. Subsequently, we considered that the less bulky borate may more readily undergo transmetallation. Gratifyingly, iodide (−)-**17** was found to be stable under basic conditions and to produce an inseparable mixture of dimeric products (d.r. = 88:12) under one-pot Suzuki coupling conditions using $Pd(OAc)_2$/SPhos[36] and *bis*(pinacolato)diboron. We subsequently attempted to establish the stereochemistry of the major atropisomer by NMR analysis and by acid-mediated deprotection of both atropisomers **19** and **20** to **1** and **23** (Fig. 4). However, both efforts failed, as the axial chirality centre is remote from existing stereocentres, leading to almost identical ^{1}H NMR spectra for both atropisomers of rugulotrosin A. Fortunately, a single crystal of the major atropisomer (−)-**19** was obtained by recrystallization (CH_2Cl_2/MeOH) from its mixture with **20**. X-ray crystal structure analysis of (−)-**19** (CCDC no.

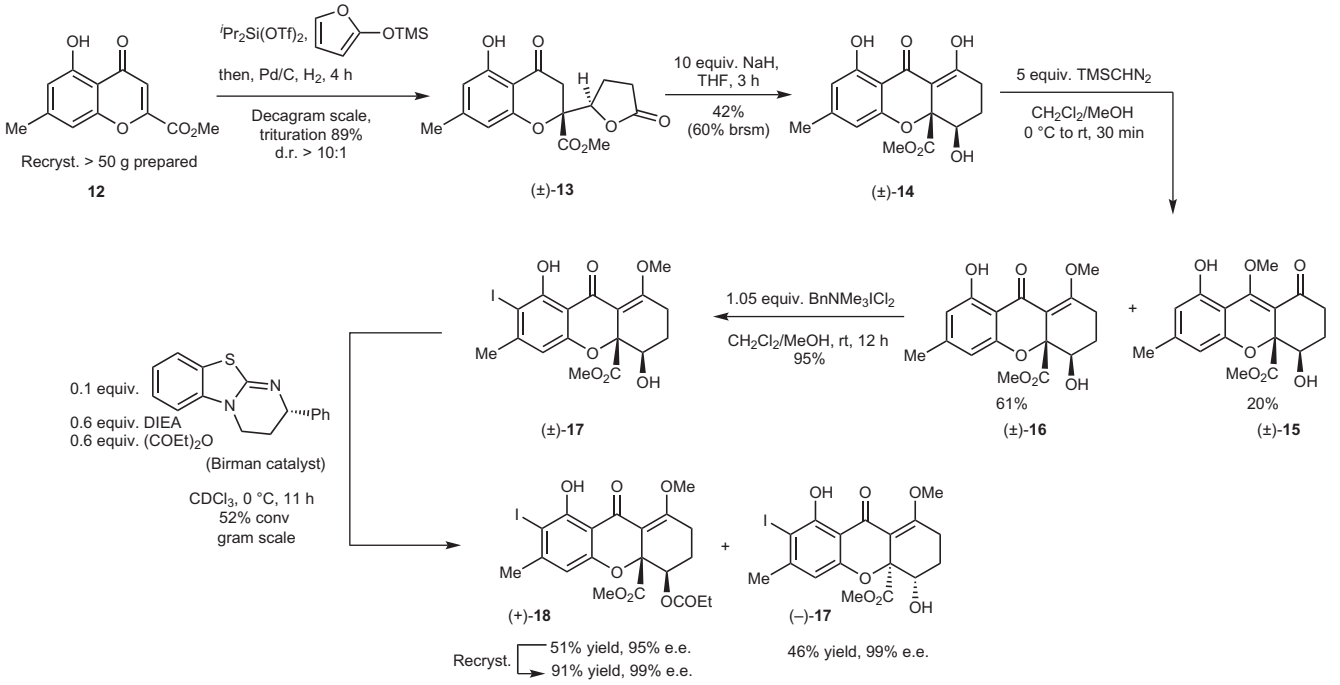

Figure 2 | Scalable syntheses of enantiopure tetrahydroxanthone monomers. Key steps involve siloxyfuran addition to a benzopyrylium species (**12** to (±)-**13**) followed by kinetic acylative resolution of (±)-**17** using the Birman catalyst.

1022610) was achieved, verifying that the relative stereochemistry was identical to that found in natural rugulotrosin A[13].

During our evaluation of dimerization conditions we found that water was essential and that the ratio of atropisomers was dependent on the ligands for palladium rather than solvent, temperature or reaction time. Accordingly, we focused our efforts on the influence of ligands on atropisomeric selectivity (Table 1). After extensive ligand screening, we found that monophosphines were crucial for the success of the reaction and that bidentate ligands such as XantPhos or DPEPhos (not shown) failed to provide the desired dimeric products. Besides SPhos (**L1**), the related ligand RuPhos (**L3**) provided dimeric products in even higher atropselectivity (93:7). Interestingly, we found when the 2′ position of the monophosphine ligand did not contain an oxygen atom (for example, a carbon atom in XPhos **L2** or a nitrogen atom in DavePhos, not shown), dimeric products were obtained in trace amounts. After experiments with achiral ligand **L4**, which provided similar results to SPhos, we anticipated that related chiral ligands may lead to efficient control of atropselectivity[37]. We began this investigation with (*R*)- and (*S*)-BI-DIME ligands **L5**[38,39], which have recently shown excellent atropselectivities in biaryl couplings. However, neither ligand was able to perform the one-pot dimerization of (–)-**12**. Gratifyingly, chiral versions of the SPhos ligands *S*-Cy-MOP (**L6**) and *R*-Cy-MOP (**L7**)[40–42] both successfully produced dimeric products. Ligand *R*-Cy-MOP provided a satisfactory d.r. (95.5:4.5) and the mismatched ligand *S*-Cy-MOP afforded a lower d.r. (81:19), both favouring the same major atropisomer. Even with the increased bulk of ligand **L8**, the d.r. did not improve noticeably. To enhance product yield, we prepared the Buchwald third-generation precatalysts[43] with SPhos, *R*-Cy-MOP and *S*-Cy-MOP. Indeed, use of the precatalyst increased yields for these cases and maintained atropselectivity. Use of *bis*(neopentyl glycolato) diboron or tetrahydroxydiboron[44,45] as boron transfer reagents led only to trace amounts of dimeric products.

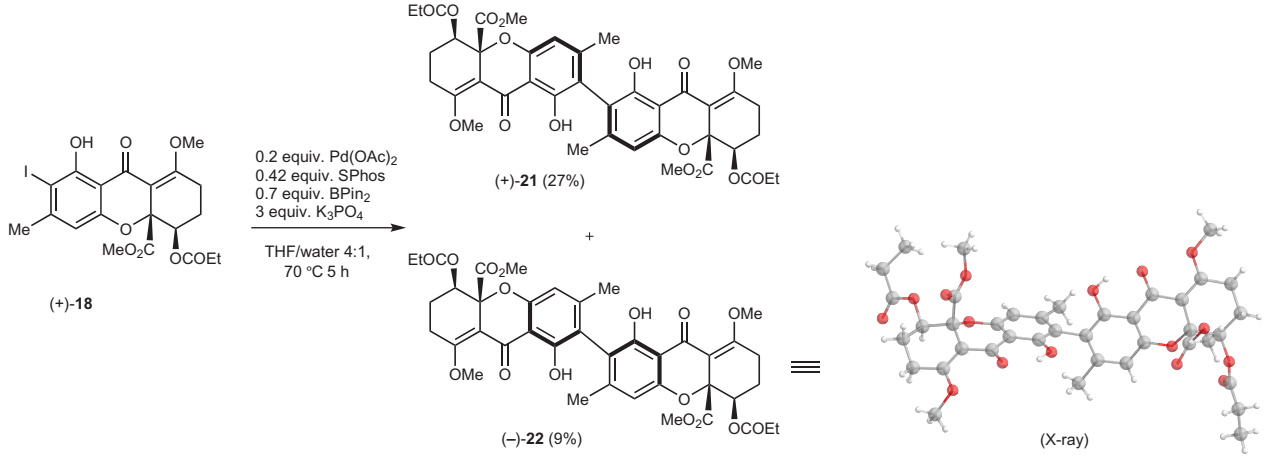

Figure 3 | One-pot Suzuki dimerization of chiral tetrahydroxanthone monomers (+)-18. Optimal conditions shown using $Pd(OAc)_2$ and SPhos as achiral ligand.

Table 1 | One-pot Suzuki dimerization of chiral tetrahydroxanthone monomer (−)-17.

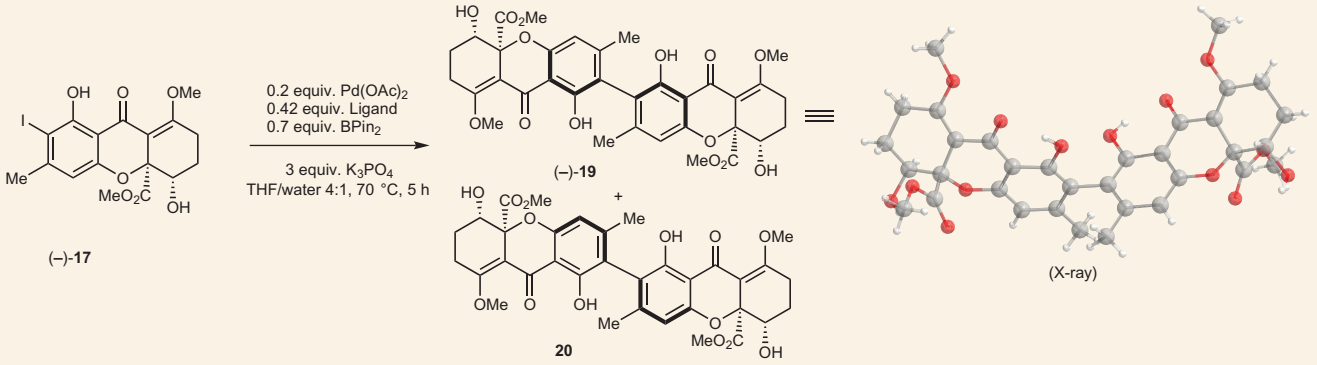

Entry	Ligand		Conversion (yield)	d.r.
1	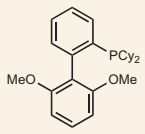	SPhos **L1**	68% (45%)	88:12
2	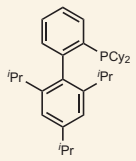	XPhos **L2**	<10% conv	
3	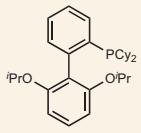	RuPhos **L3**	50% (27%)	93:7
4	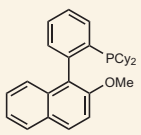	**L4**	65% (44%)	87:13
5	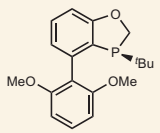	BI-DIME **L5**	No dimeric product	
6	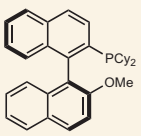	S-Cy-MOP **L6**	36% conv	81:19
7	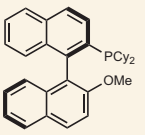	R-Cy-MOP **L7**	44% (24%)	95.5:4.5
8	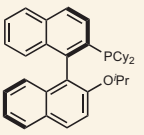	R-Cy-^{i}Pr-MOP **L8**	40% conv	90:10
9*	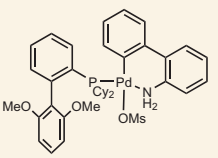	SPhos-Gen 3	72–80% (61%)	89:11
10*	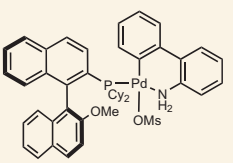	S-Cy-MOP-Gen 3	45% (~30%)	80:20
11*,†	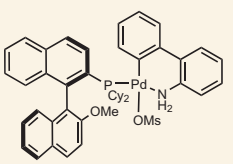	R-Cy-MOP-Gen 3	62% (44%)	95.5:4.5

*Conditions for Pd precatalyst: 0.2 equiv. Pd precatalyst, 0.7 equiv. $BPin_2$, 3 equiv. K_3PO_4, THF/water 4:1, 70 °C, 5 h; †0.6 equiv. $BPin_2$ was used.

The acylated, enantiopure monomer (+)-**18** was also investigated in the Suzuki dimerization, which generated a separable 3:1 mixture of atropisomers in 36% yield (Fig. 3). Fortunately, an X-ray crystal structure of the minor atropisomer (−)-**22** (CCDC no. 1022611) was obtained to verify the relative and absolute stereochemistry. Introduction of a bulky ester onto the secondary alcohol of the monomer (for example, OCOPh) did not affect the ratio of atropisomers.

After obtaining and establishing stereochemistry for several protected dimers, we anticipated that we could access all atropisomers and enantiomers of rugulotrosin A. Dimer (−)-**19** was treated with 3M HCl/MeOH for 10 min, which afforded rugulotrosin A ((−)-**1**) in 89% yield (Fig. 4a). In a similar manner, (+)-rugulotrosin A was obtained from acidic hydrolysis of (+)-**21** (Fig. 4b). With both enantiomers of rugulotrosin A in hand, natural rugulotrosin A was unambiguously assigned as (+)-**1** though comparison of rotation data. Similarly, *atrop*-rugulotrosin A (−)-**23** and *ent-atrop*-rugulotrosin A (+)-**23** were synthesized using similar protocols from the protected precursors (−)-**22** and (+)-**22** (Fig. 4c,d). To verify the stability of the axially chiral biaryl moiety, we heated rugulotrosin A (+)-**1** in toluene (1 mg ml^{-1}) at 100 °C for 12 h and 150 °C for 3 h. Under both conditions we did not observe the formation of *atrop*-rugulotrosin. This is supported by the high barrier of rotation of rugulotrosin A, calculated as 47.7 kcal mol^{-1} using the B3LYP/6-31G(d) level of theory (Supplementary pages 52–58).

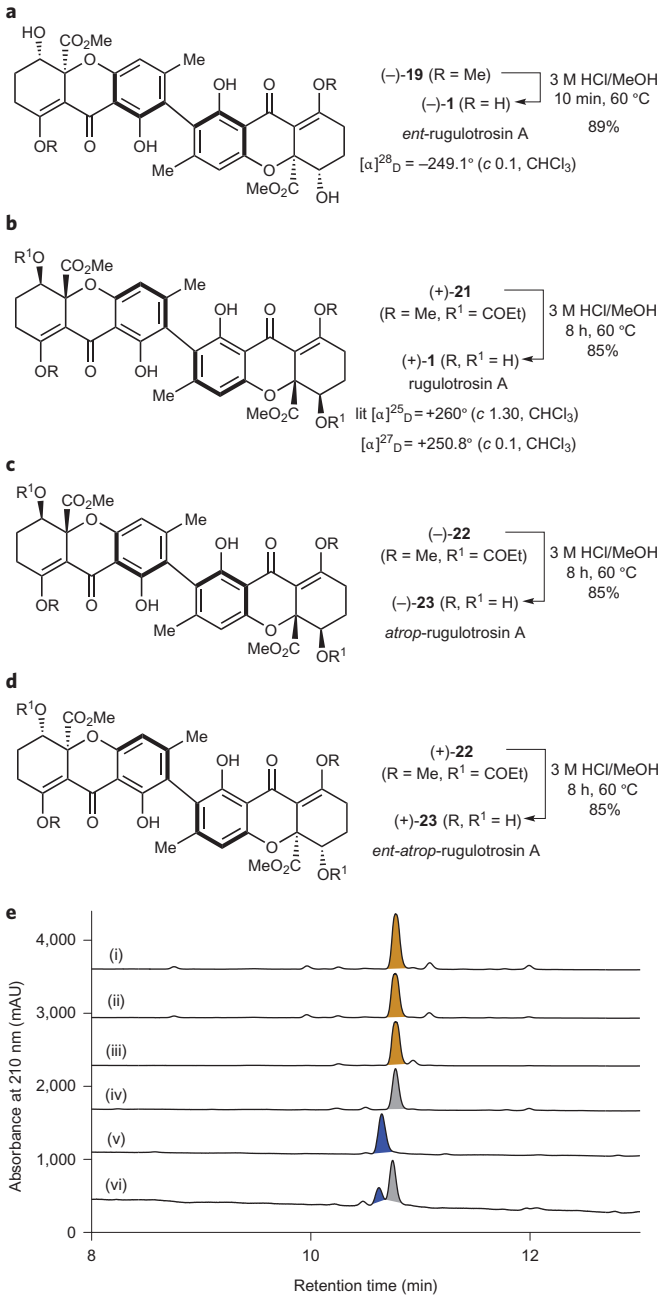

Figure 4 | Syntheses of (–) and (+)-rugulotrosin A and *atrop*-rugulotrosin A. **a**, Synthesis of *ent*-rugulotrosin A. **b**, Synthesis of rugulotrosin A and comparison rotation data with natural sample. **c**, Synthesis of *atrop*-rugulotrosin A. **d**, Synthesis of *ent-atrop*-rugulotrosin A. **e**, Comparison between the natural extract and synthetic rugulotrosins. HPLC-DAD (210 nm) (Zorbax C_{18} column, gradient elution H_2O/MeCN plus 0.05% HCO_2H) analysis of 21-day *Penicillium* nov. sp. (MST-F8741) cultures extracted with (i) MeCN or (ii) MeOH, compared against (iii) natural (+)-**1**, (iv) synthetic (+)-**1**, (v) (–)-**23** and (vi) a mixture of (+)-**1**, (–)-**1**, (–)-**23** and (+)-**23**. mAU, milli absorption units.

To rationalize the axial chirality selectivity observed in the dimerization, we modelled the geometry of the expected intermediate diaryl Pd(II) complexes[46] using SPhos (**L1**) as ligand (Fig. 5). Conformational analysis was carried out by systematic six-fold rotation about the C–Pd bonds, followed by optimization of candidate structures at the B3LYP/LanL2DZ level of theory[47]. The five lowest-energy structures are represented in Fig. 5. From this analysis, the three lowest-energy structures **24a–24c** all have dihedral angles (C1, C2, C2′, C1′) for the monomer fragments that would afford atropisomer (–)-**19** (precursor to rugulotrosin) after stereospecific reductive elimination (Fig. 5a). The next two higher energy structures **25a** and **25b** display a reversed dihedral angle that should lead to atropisomer **20** (Table 1). Relative energies correlate with the steric fit of components. Space filling models of structures **24a–c** and **25a,b** (Supplementary pages 34–52) show a more crowded arrangement of the latter, in part because of steric interactions between the methyl ester and the cyclohexyl group. The distances between the hydrogen of the methyl ester to the hydrogen on the cyclohexyl of the SPhos ligand are 2.4 and 2.5 Å for conformers **25a** and **25b**, respectively. Based on literature precedent[47], we assume that these catalyst–reactant complexes are under thermodynamic equilibration. Additional computational studies will be required to predict barriers to interconversion. It thus appears that product stereochemistry is determined by reactant and catalyst assembly in the Pd(II) complex, and this provides a basis for the prediction of stereochemistry in future atropselective couplings.

After assigning the absolute configuration of rugulotrosin A, we used our library of synthetic rugulotrosins to determine whether *Penicillium* nov. sp. (MST-F8741) was capable of producing *atrop*-rugulotrosin A. To this end, separate 21-day fermentations of MST-F8741 were extracted with either MeCN (Fig. 4e(i)) or MeOH (Fig. 4e(ii)) and were subsequently analysed using a high-performance liquid chromatography with photodiode array detection (HPLC-DAD) method optimized for the resolution of rugulotrosin A (Fig. 4e(iii,iv)) and *atrop*-rugulotrosin A (Fig. 4e (v)). To further enhance sensitivity, these analyses were also carried out using high-performance liquid chromatography with photodiode array detection and electrospray ionization mass spectrometry detection (HPLC-DAD-ESIMS) protocols augmented by single ion extraction (SIE) (Supplementary page 22). As these analytical studies failed to detect any trace of *atrop*-rugulotrosin in MST-F8741 extracts, we conclude that the rugulotrosin biosynthetic pathway present in *Penicillium* nov. sp. (MST-F8741) operates with high atropisomer fidelity.

As natural rugulotrosin A had previously been reported to exhibit antibacterial activity[13], we also tested the synthetic rugulotrosins ((+)-**1**, (–)-**1**, (–)-**23**, (+)-**23**) against several strains of Gram-positive and Gram-negative bacteria. Consistent with earlier reports, (+)-**1** exhibited antibacterial activity against *Bacillus subtilis* (ATCC 6633) (IC_{50} = 2.1 μM) and *Staphylococcus aureus* (ATCC 25923) (IC_{50} = 6 μM). Of note, enantiomer (–)-**1** was also active against *B. subtilis* (ATCC 6633) (IC_{50} = 0.7 μM) and *S. aureus* (ATCC 25923) (IC_{50} = 18 μM), whereas the antibacterial activity of the atropisomer (–)-**23** was weak and limited to *B. subtilis* (ATCC 6633) (IC_{50} = 10 μM) and (+)-**23** lacked any appreciable antibacterial activity. None of rugulotrosins (+)-**1**, (–)-**1**, (–)-**23** or (+)-**23** exhibited activity against the Gram-negative bacteria *Escherichia coli* (ATCC 25922) and *Pseudomonas aeruginosa* (ATCC 27853), nor did they exhibit cytotoxicity (IC_{50} > 30 μM) against human colon (SW620) and lung (NCI-H460) cancer cells.

Conclusion

We have developed a concise, atropselective approach to rugulotrosin A and stereoisomers through point-to-axial chirality transfer, which has facilitated the determination of the absolute configuration of rugulotrosin A. Computational studies modelling the geometry of intermediate diaryl Pd(II) complexes have provided a rationale for the atropselectivity observed in the key Suzuki dimerization. These studies highlight the utility of SPhos and related bulky monophosphine ligands[48] in palladium couplings both to bring monomers in proximity and enhance remote steric effects leading to atropselectivity. Through HPLC analysis of fungal extracts and

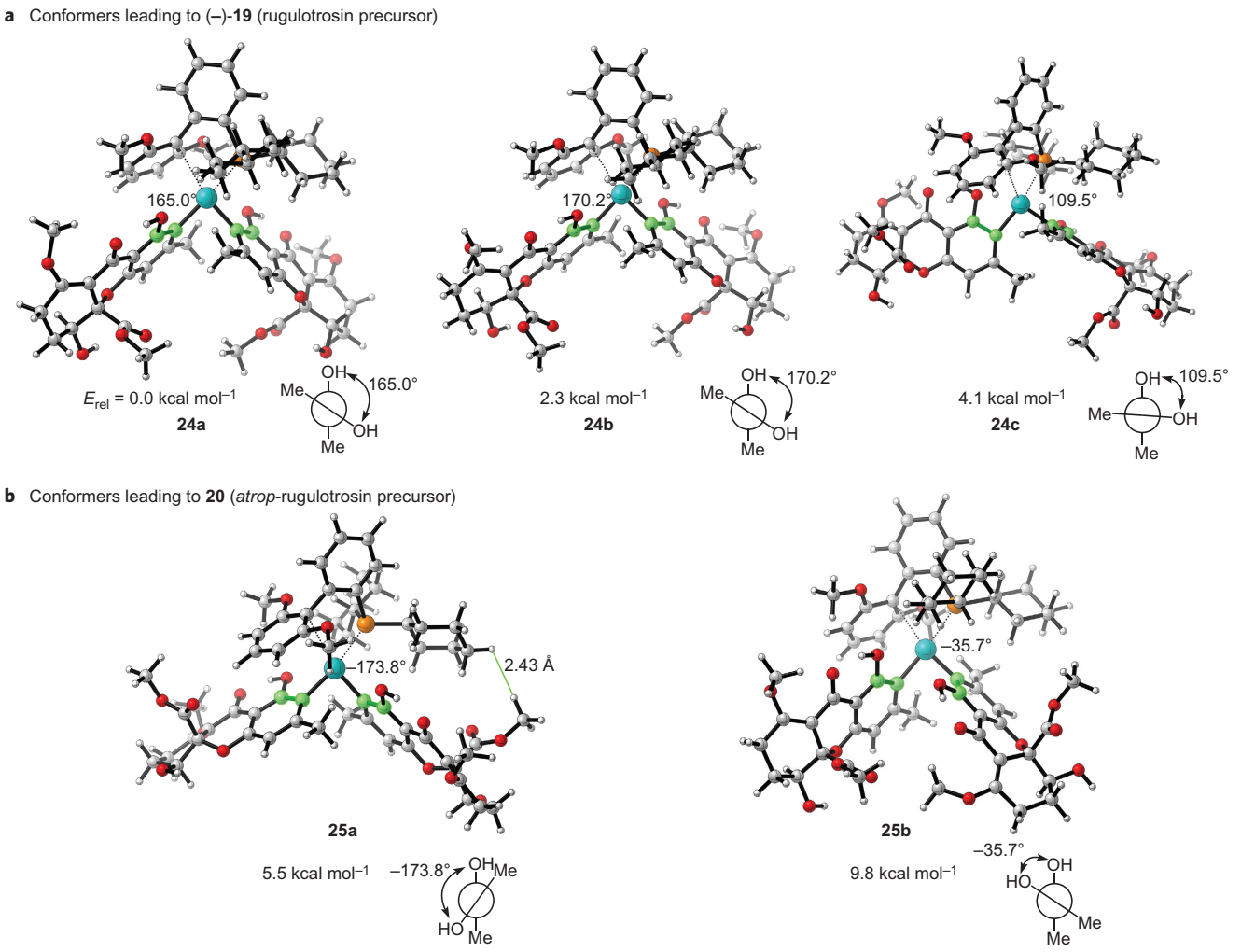

Figure 5 | Computational studies for atropselective Suzuki dimerization. Conformational analysis was optimized at the B3LYP/LanL2DZ level of theory. Dihedral angles were measured by C1, C2, C2′ and C1′ and are shown in green. **a**, Conformers leading to (–)-**19**. **b**, Conformers leading to **20**.

synthetic samples, we have determined that *Penicillium* nov. sp. (MST-F8741) generates rugulotrosin A in an atropselective manner. Moreover, the atropisomers and enantiomers of rugulotrosin A were found to have different activities against Gram-positive bacteria, illustrating the importance of stereochemistry on target selectivity. Further studies regarding atropselective syntheses of dimeric natural products are currently under investigation and will be reported in due course.

Received 29 September 2014; accepted 16 December 2014; published online 2 February 2015

References

1. Moss, G. P. Basic terminology of stereochemistry. *Pure Appl. Chem.* **68,** 2193–2222 (1996).
2. Zask, A., Murphy, J. & Ellestad, G. A. Biological stereoselectivity of atropisomeric natural products and drugs. *Chirality* **25,** 265–274 (2013).
3. Clayden, J., Moran, W. J., Edwards, P. J. & LaPlante, S. R. The challenge of atropisomerism in drug discovery. *Angew. Chem. Int. Ed.* **48,** 6398–6401 (2009).
4. LaPlante, S. R., Edwards, P. J., Fader, L. D., Jakalian, A. & Hucke, O. Revealing atropisomer axial chirality in drug discovery. *ChemMedChem* **6,** 505–513 (2011).
5. Bringmann, G. *et al.* Atroposelective synthesis of axially chiral biaryl compounds. *Angew. Chem. Int. Ed.* **44,** 5387–5427 (2005).
6. Bringmann, G., Gulder, T., Gulder, T. A. M. & Breuning, M. Atroposelective total synthesis of axially chiral biaryl natural products. *Chem. Rev.* **111,** 563–639 (2011).
7. Kozlowski, M. C., Morgan, B. J. & Linton, E. C. Total synthesis of chiral biaryl natural products by asymmetric biaryl coupling. *Chem. Soc. Rev.* **38,** 3193–3207 (2009).
8. Liau, B. B., Milgram, B. C. & Shair, M. D. Total syntheses of HMP-Y1, hibarimicinone, and HMP-P1. *J. Am. Chem. Soc.* **134,** 16765–16772 (2012).
9. Masters, K-S. & Bräse, S. Xanthones from fungi, lichens, and bacteria: the natural products and their synthesis. *Chem. Rev.* **112,** 3717–3776 (2012).
10. Wezeman, T., Masters, K-S. & Bräse, S. Double trouble—the art of synthesis of chiral dimeric natural products. *Angew. Chem. Int. Ed.* **53,** 4524–4526 (2014).
11. Franck, B., Gottschalk, E. M., Ohnsorge, U. & Baumann, G. The structure of secalonic acids A and B. *Angew. Chem. Int. Ed. Engl.* **3,** 441–442 (1964).
12. Steyn, P. S. The isolation, structure and absolute configuration of secalonic acid D, the toxic metabolite of *Penicillium oxalicum*. *Tetrahedron* **26,** 51–57 (1970).
13. Stewart, M. *et al.* Rugulotrosins A and B: two new antibacterial metabolites from an Australian isolate of a *Penicillium* sp. *J. Nat. Prod.* **67,** 728–730 (2004).
14. Kikuchi, H., Isobe, M., Kurata, S., Katou, Y. & Oshima, Y. New dimeric and monomeric chromanones, gonytolides D-G, isolated from the fungus *Gonytrichum* sp. *Tetrahedron* **68,** 6218–6223 (2012).
15. Kikuchi, H. *et al.* Structures of the dimeric and monomeric chromanones, gonytolides A–C, isolated from the fungus *Gonytrichum* sp. and their promoting activities of innate immune responses. *Org. Lett.* **13,** 4624–4627 (2011).
16. Nicolaou, K. C. & Li, A. Total syntheses and structural revision of α- and β-diversonolic esters and total syntheses of diversonol and blennolide C. *Angew. Chem. Int. Ed.* **47,** 6579–6582 (2008).
17. Tietze, L. F. *et al.* Enantioselective total synthesis of (–)-diversonol. *Chem. Eur. J.* **19,** 4876–4882 (2013).

18. Tietze, L. F., Ma, L., Reiner, J. R., Jackenkroll, S. & Heidemann, S. Enantioselective total synthesis of (−)-blennolide A. *Chem. Eur. J.* **19,** 8610–8614 (2013).
19. Tietze, L. F., Jackenkroll, S., Hierold, J., Ma, L. & Waldecker, B. A domino approach to the enantioselective total syntheses of blennolide C and gonytolide C. *Chem. Eur. J.* **20,** 8628–8635 (2014).
20. Nising, C. F., Ohnemüller, U. K. & Bräse, S. The total synthesis of the fungal metabolite diversonol. *Angew. Chem. Int. Ed.* **45,** 307–309 (2006).
21. Meister, A. C. *et al.* Total synthesis of blennolide mycotoxins: design, synthetic routes and completion. *Eur. J. Org. Chem.* 4861–4875 (2014).
22. Qin, T., Johnson, R. P. & Porco, J. A. Jr Vinylogous addition of siloxyfurans to benzopyryliums: a concise approach to the tetrahydroxanthone natural products. *J. Am. Chem. Soc.* **133,** 1714–1717 (2011).
23. Qin, T. & Porco, J. A. Jr Total syntheses of secalonic acids A and D. *Angew. Chem. Int. Ed.* **53,** 3107–3110 (2014).
24. Wilson, J. M. & Cram, D. J. Chiral leaving groups induce asymmetry in syntheses of binaphthyls in nucleophilic aromatic substitution reactions. *J. Am. Chem. Soc.* **104,** 881–884 (1982).
25. Evans, D. A. *et al.* Nonconventional stereochemical issues in the design of the synthesis of the vancomycin antibiotics: challenges imposed by axial and nonplanar chiral elements in the heptapeptide aglycons. *Angew. Chem. Int. Ed.* **37,** 2704–2708 (1998).
26. Burns, N. Z., Krylova, Z. N., Hanroush, R. N. & Baran, P. S. Scalable total synthesis and biological evaluation of haouamine A and its atropisomer. *J. Am. Chem. Soc.* **131,** 9172–9173 (2009).
27. Guo, F., Konkol, L. C. & Thomson, R. J. Enantioselective synthesis of biphenols from 1,4-diketones by traceless central-to-axial chirality exchange. *J. Am. Chem. Soc.* **133,** 18–20 (2011).
28. Konkol, L. C., Guo, F., Sarjeant, A. A. & Thomson, R. J. Enantioselective total synthesis and studies into the configurational stability of bismurrayaquinone A. *Angew. Chem. Int. Ed.* **50,** 9931–9934 (2011).
29. Park, Y. S. *et al.* Synthesis of (−)-viriditoxin: a 6,6′-binaphthopyran-2-one that targets the bacterial cell division protein FtsZ. *Angew. Chem. Int. Ed.* **50,** 3730–3733 (2011).
30. Lipshutz, B. H. & Keith, L. M. A stereospecific, intermolecular biaryl-coupling approach to korupensamine A en route to the michellamines. *Angew. Chem. Int. Ed.* **38,** 3530–3533 (1999).
31. Huang, S., Peterson, T. B. & Lipshutz, B. H. Total synthesis of (+)-korupensamine B via an atropselective intermolecular biaryl coupling. *J. Am. Chem. Soc.* **132,** 14021–14023 (2010).
32. Coleman, R. S. & Grant, E. B. Atropdiastereoselective total synthesis of phleichrome and the protein kinase C inhibitor calphostin A. *J. Am. Chem. Soc.* **116,** 8795–8796 (1994).
33. Broka, C. A. Total syntheses of phleichrome, calphostin A, and calphostin D. Unusual stereoselective and stereospecific reactions in the synthesis of perylenequinones. *Tetrahedron Lett.* **32,** 859–862 (1991).
34. Birman, V. B. & Li, X. Homobenzotetramisole: an effective catalyst for kinetic resolution of aryl-cycloalkanols. *Org. Lett.* **10,** 1115–1118 (2008).
35. Müller, C. E. & Schreiner, P. R. Organocatalytic enantioselective acyl transfer onto racemic as well as *meso* alcohols, amines, and thiols. *Angew. Chem. Int. Ed.* **50,** 6012–6042 (2010).
36. Barder, T. E., Walker, S. D., Martinelli, J. R. & Buchwald, S. L. Catalysts for Suzuki–Miyaura coupling processes: scope and studies of the effect of ligand structure. *J. Am. Chem. Soc.* **127,** 4685–4696 (2005).
37. Masamune, S., Choy, W., Petersen, J. S. & Sita, L. R. Double asymmetric synthesis and a new strategy for stereochemical control in organic synthesis. *Angew. Chem. Int. Ed. Engl.* **24,** 1–30 (1985).
38. Tang, W. *et al.* A general and special catalyst for Suzuki–Miyaura coupling processes. *Angew. Chem. Int. Ed.* **49,** 5879–5883 (2010).
39. Xu, G., Fu, W., Liu, G., Senanayake, C. H. & Tang, W. Efficient syntheses of korupensamines A, B and michellamine B by asymmetric Suzuki–Miyaura coupling reactions. *J. Am. Chem. Soc.* **136,** 570–573 (2014).
40. Hamada, T., Chieffi, A., Ahman, J. & Buchwald, S. L. An improved catalyst for the asymmetric arylation of ketone enolates. *J. Am. Chem. Soc.* **124,** 1261–1268 (2002).
41. Zhou, Y. *et al.* Enantioselective synthesis of axially chiral multifunctionalized biaryls via asymmetric Suzuki–Miyaura coupling. *Org. Lett.* **15,** 5508–5511 (2013).
42. Zhou, Y. *et al.* Enantioselective synthesis of axially chiral biaryl monophosphine oxides via direct asymmetric Suzuki coupling and DFT investigations of the enantioselectivity. *ACS Catal.* **4,** 1390–1397 (2014).
43. Bruno, N. C., Tudge, M. T. & Buchwald, S. L. Design and preparation of new palladium precatalysts for C–C and C–N cross-coupling reactions. *Chem. Sci.* **4,** 916–920 (2013).
44. Little, S. & Trice, J. in *Encyclopedia of Reagents for Organic Synthesis* (Wiley, 2001); http://onlinelibrary.wiley.com/doi/10.1002/047084289X.rn01181/abstract
45. Molander, G. A., Trice, S. L. J., Kennedy, S. M., Dreher, S. D. & Tudge, M. T. Scope of the palladium-catalyzed aryl borylation utilizing *bis*-boronic acid. *J. Am. Chem. Soc.* **134,** 11667–11673 (2012).
46. Gensch, T. *et al.* Snapshot of the palladium (II)-catalyzed oxidative biaryl bond formation by X-ray analysis of the intermediate diaryl palladium (II) complex. *Chem. Eur. J.* **18,** 770–776 (2012).
47. Shen, X., Jones, G. O., Watson, D. A., Bhayana, B. & Buchwald, S. L. Enantioselective synthesis of axially chiral biaryls by the Pd-catalyzed Suzuki–Miyaura reaction: substrate scope and quantum mechanical investigation. *J. Am. Chem. Soc.* **132,** 11278–11287 (2010).
48. Martin, R. & Buchwald, S. L. Palladium-catalyzed Suzuki–Miyaura cross-coupling reactions employing dialkylbiaryl phosphine ligands. *Acc. Chem. Res.* **41,** 1461–1473 (2008).

Acknowledgements

Financial support from the National Institutes of Health (NIH, GM-099920) and Vertex Pharmaceuticals, Inc. (graduate fellowship to T.Q.) is gratefully acknowledged. The authors thank J. Bacon for crystal structure determination, B. Qu and C. Senanayake for providing both (*R*) and (*S*)-BI-DIME ligands and E. Lacey for supplying extracts of *Penicillium* nov. sp. (MST-F8741). Research at the BU-CMD was supported by the NIH (grant GM-067041). This work used the Extreme Science and Engineering Discovery Environment (XSEDE), which is supported by the National Science Foundation (grant OCI-1053575).

Author contributions

T.Q. and J.A.P. Jr conceived of the project, designed and carried out the experiments, analysed the data and wrote most of the paper. S.L.S-J. and R.P.J. performed computational studies. Z.G.K. and R.J.C. performed natural extract comparisons and biological studies. All authors discussed the results and commented on the manuscript.

Additional information

Supplementary information and chemical compound information are available in the online version of the paper. Reprints and permissions information is available online at www.nature.com/reprints. Correspondence and requests for materials should be addressed to J.A.P. Jr.

Competing financial interests

The authors declare no competing financial interests.